Manifestation of the Gouy phase in strongly focused, radially polarized beams

Xiaoyan Pang[1] **and Taco D. Visser**[1,2*]

[1]*Faculty of Electrical Engineering, Mathematics and Computer Science, Delft University of Technology, Delft, The Netherlands*
[2]*Department of Physics and Astronomy, and Institute for Lasers, Life and Biophotonics, VU University, Amsterdam, The Netherlands*
[*]*T.D. Visser@tudelft.nl*

Abstract: The Gouy phase, sometimes called the focal phase anomaly, is the curious effect that in the vicinity of its focus a diffracted field, compared to a non-diffracted, converging spherical wave of the same frequency, undergoes a rapid phase change by an amount of π. We theoretically investigate the phase behavior and the polarization ellipse of a strongly focused, radially polarized beam. We find that the significant variation of the state of polarization in the focal region, is a manifestation of the different Gouy phases that the two electric field components undergo.

OCIS codes: (050.1960) Diffraction theory; (260.1960) Diffraction theory; (260.2110) Electromagnetic optics; (260.5430) Polarization.

References and links

1. L. G. Gouy, "Sur une propriété nouvelle des ondes lumineuses," Comptes Rendus hebdomadaires des Séances de l'Académie des Sciences **110**, 1251–1253 (1890).
2. L. G. Gouy, "Sur la propagation anomale des ondes," Annales des Chimie et de Physique **24**, 145–213 (1891).
3. S. M. Baumann, D. M. Kalb, and E. J. Galvez, "Propagation dynamics of optical vortices due to Gouy phase," Opt. Express **17**, 9818–9827 (2009).
4. G. M. Philip, V. Kumar, G. Milione, and N. K. Viswanathan, "Manifestation of the Gouy phase in vector-vortex beams," Opt. Lett. **37**, 2667–2669 (2012).
5. W. Zhu, A. Agrawal, A. Nahata, "Direct measurement of the Gouy phase shift for surface plasmon-polaritons," Opt. Express **15**, 9995–10001 (2007).
6. T. D. Visser and E. Wolf, "The origin of the Gouy phase anomaly and its generalization to astigmatic wavefields," Opt. Commun. **283**, 3371–3375 (2010).
7. M. W. Beijersbergen, L. Allen, H. E. L. O. van der Veen, and J. P. Woerdman, "Astigmatic laser mode converters and transfer of orbital angular momentum," Opt. Commun. **96**, 123–132 (1993).
8. G. Lamouche, M. L. Dufour, B. Gauthier and J.-P. Monchalin, "Gouy phase anomaly in optical coherence tomography," Opt. Commun. **239**, 297–301 (2004).
9. T. Klaassen, A. Hoogeboom, M. P. van Exter and J. P. Woerdman, "Gouy phase of nonparaxial eigenmodes in a folded resonator," J. Opt. Soc. Am. A **21**, 1689–1693 (2004).
10. X. Pang, D. G. Fischer and T. D. Visser, "A generalized Gouy phase for focused partially coherent light and its implications for interferometry," J. Opt. Soc. Am. A **29**, 989–993. (2012).
11. X. Pang, T. D. Visser and E. Wolf, "Phase anomaly and phase singularities of the field in the focal region of high-numerical aperture systems," Opt. Commun. **284**, 5517–5522 (2011).
12. K. S. Youngworth and T. G. Brown, "Focusing of high numerical aperture cylindrical-vector beams," Opt. Express **7**, 77–87 (2000).
13. R. Martínez-Herrero and P. M. Mejías, "Propagation and parametric characterization of the polarization structure of paraxial radially and azimuthally polarized beams," Opt. Laser Techn. **44**, 482–485 (2012).
14. R. Dorn and S. Quabis and G. Leuchs, "Sharper focus for a radially polarized light beam," Phys. Rev. Lett. **91**, 233901 (2003).

#184950 - $15.00 USD Received 5 Feb 2013; revised 19 Mar 2013; accepted 21 Mar 2013; published 28 Mar 2013

15. L. Novotny, M. R. Beversluis, K. S. Youngworth and T. G. Brown, "Longitudinal field modes probed by single molecules," Phys. Rev. Lett. **86**, 5251–5254 (2001).
16. C. J. R. Sheppard and A. Choudhury, "Annular pupils, radial polarization, and superresolution," Appl. Opt. **43**, 4322–4327 (2004).
17. Q. Zhan, "Trapping metallic Rayleigh particles with radial polarization," Opt. Express **12**, 3377–3382 (2004).
18. T. A. Nieminen, N. R. Heckenberg and H. Rubinsztein-Dunlop, "Forces in optical tweezers with radially and azimuthally polarized trapping beams," Opt. Lett. **33**, 122–124 (2008).
19. D. P. Biss, K. S. Youngworth and T. G. Brown, "Dark-field imaging with cylindrical-vector beams," Appl. Opt. **45**, 470–479 (2006).
20. T. G. Brown "Unconventional polarization states: Beam propagation, focusing, and imaging," in *Progress in Optics*, E. Wolf eds. (Elsevier, 2011), **56**, pp. 81–129.
21. T. D. Visser and J. T. Foley, "On the wavefront spacing of focused, radially polarized beams," J. Opt. Soc. Am. A **22**, 2527–2531 (2005).
22. H. Chen, Q. Zhan, Y. Zhang, and Y.-P. Li, "The Gouy phase shift of the highly focused radially polarized beam," Phys. Lett. A **371**, 259–261 (2007).
23. B. Richards and E. Wolf, "Electromagnetic diffraction in optical systems, II. Structure of the image field in aplanatic systems," Proc. R. Soc. London Ser. A **253**, 358–379 (1959).
24. M. Born and E. Wolf, *Principles of Optics: Electromagnetic Theory of Propagation, Interference and Diffraction of Light*, Seventh (expanded) edition (Cambridge University Press, 1999).
25. M. Abramowitz and I.A. Stegun, *Handbook of Mathematical Functions with Formulas, Graphs, and Mathematical Tables* (Dover, 1965).
26. R.W. Schoonover and T.D. Visser, "Polarization singularities of focused, radially polarized fields," Opt. Express **14**, 5733–5745 (2006).
27. R. Martínez-Herrero and P.M. Mejías, "Stokes-parameters representation in terms of the radial and azimuthal field components: A proposal ," Opt. Laser Techn. **42**, 1099–1102 (2010).
28. G.J. Gbur, *Mathematical Methods for Optical Physics and Engineering* (Cambridge University Press, Cambridge, 2011), pp. 91–93.
29. D.W. Diehl, R.W. Schoonover and T.D. Visser, "The structure of focused, radially polarized fields," Opt. Express **14**, 3030–3038 (2006).

1. Introduction

The phase anomaly is a measure of how the phase of a monochromatic, focused wave field differs from that of a non-diffracted, converging spherical wave of the same frequency. Since its first description by L.G. Gouy in the 1890s [1, 2], his namesake phase has been observed under a wide variety of circumstances. Recently investigated systems range from vortex beams [3, 4] to fields of surface plasmon polaritions [5]. Surprisingly many different explanations for the physical origin of this remarkable effect have been suggested (see [6] and the references therein). Because of its crucial role in many applications such as mode conversion [7], coherence tomography [8], the tuning of the resonance frequency of laser cavities [9], and interference microscopy [10], the Gouy phase continues to attract attention.

When a beam of light is focused by a high-aperture system, the usual scalar formalism no longer suffices, and an analysis of the Gouy phase must then take the vector nature of the field into account. This has recently been done for strongly focused, linearly polarized beams [11]. It was found that the Gouy phases of the three Cartesian components of the electric field exhibit quite different behaviors. Another example which requires a vectorial description is the focusing of radially polarized beams [12, 13]. Because of their intriguing properties, such as a relatively small focal spot size [14], these beams are widely used in, for example, the probing of the dipole moment of individual molecules [15], high-resolution microscopy [16], trapping of strongly scattering particles [17, 18] and in dark-field imaging [19]. A review is presented in [20].

A first indication of the complicated phase behavior of focused, radially polarized beams was the observation that their wave spacing near focus is highly irregular [21]. This was followed by a study of the Gouy phase of the longitudinal component of the electric field vector at the focal plane [22]. In the present paper, the Gouy phase of the total electric field vector,

#184950 - $15.00 USD Received 5 Feb 2013; revised 19 Mar 2013; accepted 21 Mar 2013; published 28 Mar 2013

consisting of a radial and longitudinal component, is examined in the entire focal region. It is found that the strong changes in the shape and orientation of the polarization ellipse near focus is a consequence of the different Gouy phases that these two components undergo.

2. Focused, radially polarized fields

Consider an aplanatic focusing system L of focal length f with a semi-aperture angle α. The

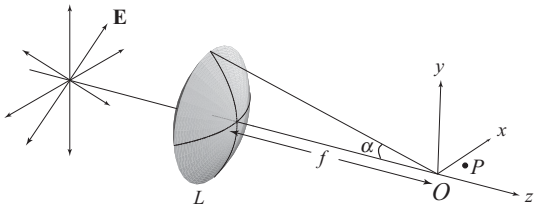

Fig. 1. A high-numerical-aperture focusing system with an incident beam that is radially polarized.

geometrical focus is indicated by O and is taken to be the origin of a Cartesian coordinate system (see Fig. 1). A monochromatic, radially polarized beam with angular frequency ω is incident upon the system. The electric and magnetic fields at time t at position $\mathbf{r}$ are given by the expressions

$$\mathbf{E}(\mathbf{r},t) = \mathrm{Re}\left[\mathbf{e}(\mathbf{r})\exp(-\mathrm{i}\omega t)\right], \tag{1}$$

$$\mathbf{H}(\mathbf{r},t) = \mathrm{Re}\left[\mathbf{h}(\mathbf{r})\exp(-\mathrm{i}\omega t)\right], \tag{2}$$

respectively, where Re denotes the real part. Such a field may be generated, for example, by the superposition of two, mutually orthogonally polarized, Hermite-Gaussian beams. In the remainder we will only be concerned with the electric field. If we assume that the entrance plane of the focusing system coincides with the waist plane of the beam, then the longitudinal component e_z and the radial component e_ρ of the electric field at a point $P=(\rho,z)$ in the focal region are given by the equations (first derived in [12], but here we adopt the notation of [21])

$$e_z(\rho,z) = -\mathrm{i}kf\int_0^\alpha l(\theta)\sin^2\theta\cos^{1/2}\theta e^{\mathrm{i}kz\cos\theta}J_0(k\rho\sin\theta)\,\mathrm{d}\theta, \tag{3}$$

$$e_\rho(\rho,z) = -kf\int_0^\alpha l(\theta)\sin\theta\cos^{3/2}\theta e^{\mathrm{i}kz\cos\theta}J_1(k\rho\sin\theta)\,\mathrm{d}\theta, \tag{4}$$

where J_i is the Bessel function of the first kind of order i and $k=\omega/c$, with c the speed of light in vacuum, is the wavenumber associated with frequency ω. Furthermore, $l(\theta)$ denotes the angular amplitude function

$$l(\theta) = f\sin\theta\exp[-f^2\sin^2\theta/\omega_0^2], \tag{5}$$

where ω_0 is the spot size of the beam in the waist plane. Note that since the incident electric field has no azimuthal component and the configuration is invariant with respect to rotations around the z-axis, there is no azimuthal component of the electric field in the focal region. The position of an observation point may be indicated by the dimensionless Lommel variables u and v [23], namely

$$u = kz\sin^2\alpha, \tag{6}$$

$$v = k\rho\sin\alpha. \tag{7}$$

#184950 - $15.00 USD Received 5 Feb 2013; revised 19 Mar 2013; accepted 21 Mar 2013; published 28 Mar 2013

Equations (3) and (4) can then be rewritten as

$$e_z(u,v) = -\mathrm{i}kf^2\int_0^\alpha \sin^3\theta\cos^{1/2}\theta\; e^{-\beta^2\sin^2\theta}e^{\mathrm{i}u\cos\theta/\sin^2\alpha}J_0\left(\frac{v\sin\theta}{\sin\alpha}\right)\mathrm{d}\theta, \quad (8)$$

$$e_\rho(u,v) = -kf^2\int_0^\alpha \sin^2\theta\cos^{3/2}\theta\; e^{-\beta^2\sin^2\theta}e^{\mathrm{i}u\cos\theta/\sin^2\alpha}J_1\left(\frac{v\sin\theta}{\sin\alpha}\right)\mathrm{d}\theta, \quad (9)$$

where

$$\beta = f/\omega_0, \quad (10)$$

denotes the ratio of the focal length of the system and the spot size of the beam in the waist plane.

It follows from Eqs. (8) and (9) that the field components obey the following symmetry relations:

$$e_z(-u,v) = -e_z^*(u,v), \quad (11)$$

$$e_\rho(-u,v) = e_\rho^*(u,v). \quad (12)$$

3. Two Gouy phases

The Gouy phase δ is defined as the difference between the actual phase of the field and that of a (non-diffracted) spherical wave converging to the focus in the half-space $z<0$ and diverging from it in the half-space $z>0$ ([24, Sec. 8.8, Eq. (48)]). For each individual component of the electric field we therefore define a Gouy phase as

$$\delta_z(u,v) = \arg[e_z(u,v)] - \mathrm{sign}(u)kR, \quad (13)$$

$$\delta_\rho(u,v) = \arg[e_\rho(u,v)] - \mathrm{sign}(u)kR, \quad (14)$$

where R is the distance from the observation point to the geometrical focus, i.e.

$$kR = k\sqrt{z^2+\rho^2} = \frac{1}{\sin\alpha}\sqrt{\frac{u^2}{\sin^2\alpha}+v^2}, \quad (15)$$

and $\mathrm{sign}(x)$ denotes the sign function

$$\mathrm{sign}(x) = \begin{cases} -1 & \text{if } x<0, \\ 1 & \text{if } x>0. \end{cases} \quad (16)$$

For the longitudinal field component e_z, one finds from Eqs. (8), (11) and (13) that the Gouy phase at two points that are symmetrically located with respect to the focus satisfies the relation

$$\delta_z(-u,v)+\delta_z(u,v) = -\pi \pmod{2\pi}. \quad (17)$$

At the focus we have

$$\delta_z(0,0) = -\pi/2 \pmod{2\pi}. \quad (18)$$

For the radial field component e_ρ, it follows from Eqs. (9), (12) and (14) that the Gouy phase satisfies the symmetry relations

$$\delta_\rho(-u,v)+\delta_\rho(u,v) = 0 \pmod{2\pi}. \quad (19)$$

#184950 - $15.00 USD Received 5 Feb 2013; revised 19 Mar 2013; accepted 21 Mar 2013; published 28 Mar 2013

Even though $e_\rho = 0$ when $v = 0$, it is useful to study the behavior of δ_ρ along a tilted ray through focus; for such a ray $v \propto |u|$. Using the fact that for small arguments $J_n(x) \sim x^n$ [25, p. 360] we find from Eq. (9) that along a tilted ray $e_\rho \sim -|u|$. Hence

$$\lim_{u\downarrow 0} \delta_\rho(u,v) = \lim_{u\uparrow 0} \delta_\rho(u,v) = \pi \pmod{2\pi}. \tag{20}$$

It is seen from Eqs. (8) and (9) that the electric field components are characterized by two parameters, namely the semi-aperture angle α, and the beam-size parameter β. These two parameters have a different effect on the Gouy phase behavior as we will now demonstrate.

On the central axis of the system ($v = 0$) only the longitudinal field component e_z is non-zero. The Gouy phase pertaining to this component, δ_z, is shown in Fig. 2 for various values of the semi-aperture angle α. It is seen that the phase change of e_z decreases as α increases. Unlike the π phase jump of the longitudinal component in linearly polarized fields [11], the Gouy phase here is continuous at focus. Note that the longitudinal coordinate u is dependent on the value of the semi-aperture angle α [See Eq. (6)].

In Fig. 3 the Gouy phase δ_z is depicted for selected values of the beam-size parameter β. For a decreasing beam waist-size (ω_0) the Gouy phase decreases as well. In these two figures, the negative or positive slope of the Gouy phase means that the wavefront spacings can be smaller or bigger than λ. This effect has been discussed in [21].

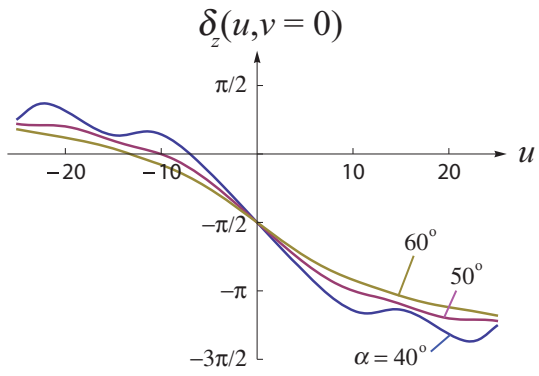

Fig. 2. The Gouy phase δ_z along the optical axis ($v = 0$) of the electric field component e_z for selected values of the semi-aperture angle α (blue curve: $\alpha = 40^\circ$, red curve: $\alpha = 50^\circ$, olive curve: $\alpha = 60^\circ$). The beam-size parameter $\beta = 3$.

When $v \neq 0$, it follows from Eqs. (8) and (9) that both the longitudinal component e_z and the radial component e_ρ contribute to the field. The two Gouy phases δ_z and δ_ρ along an oblique ray through focus, which makes an angle $\theta = 35^\circ$ with the z-axis, are shown in Fig. 4. It is clear that their respective behaviors are quite different. For example, when $-10 < u < -5$ the oscillations of δ_z and δ_ρ are out of phase. The implications of this effect for the state of polarization will be discussed in the next section.

4. The Gouy phase and the state of polarization

It is convenient to characterize the state of polarization of a two-dimensional field by the four Stokes parameters [24, Sec. 1.4]. For a beam propagating in the z-direction, these parameters are defined in terms of e_x and e_y. For a focused, radially polarized field the two non-zero components of the electric field are e_z and e_ρ. It is natural, therefore, to define the Stokes parameters

#184950 - $15.00 USD Received 5 Feb 2013; revised 19 Mar 2013; accepted 21 Mar 2013; published 28 Mar 2013

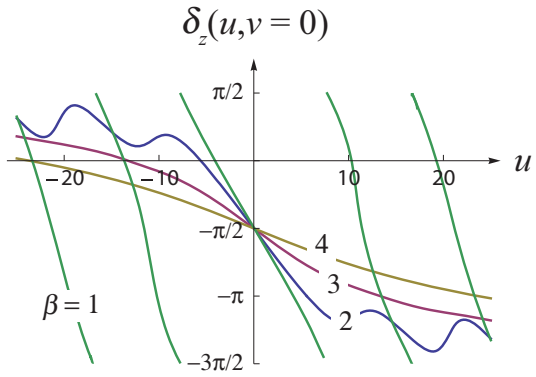

Fig. 3. The Gouy phase δ_z along the optical axis ($v = 0$) of the electric field component e_z for selected values of the beam-size parameter $\beta = f/\omega_0$ (green curve: $\beta = 1$, blue curve: $\beta = 2$, red curve: $\beta = 3$, olive curve: $\beta = 4$). The semi-aperture angle $\alpha = 60^\circ$.

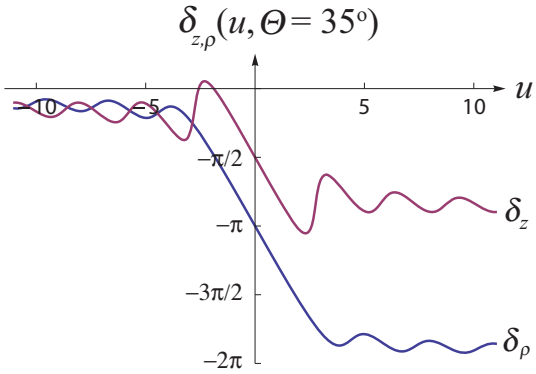

Fig. 4. The Gouy phase of the longitudinal component e_z (red curve) and that of the radial component e_ρ (blue curve) along an oblique ray through focus under an angle $\theta = 35^\circ$. Here $\alpha = 40^\circ$ and $\beta = 1$.

in this case in terms of these components rather than e_x and e_y [26, 27]. We thus define

$$S_0 = |e_z|^2 + |e_\rho|^2, \tag{21}$$
$$S_1 = |e_z|^2 - |e_\rho|^2, \tag{22}$$
$$S_2 = 2|e_z||e_\rho|\cos\delta, \tag{23}$$
$$S_3 = 2|e_z||e_\rho|\sin\delta, \tag{24}$$

where $\delta = \arg[e_z] - \arg[e_\rho] = \delta_z - \delta_\rho$. The normalized form of these Stokes parameters, $s_1 = S_1/S_0$, $s_2 = S_2/S_0$, $s_3 = S_3/S_0$, represents a point on the Poincaré sphere [28, p. 316], as shown in Fig. 5. On the northern hemisphere ($s_3 > 0$), the polarization is right-handed (clockwise), whereas on the southern hemisphere it is left-handed (counter-clockwise). On both poles ($s_3 = \pm 1$), the polarization is circular. On the equator ($s_3 = 0$), the field is linearly polarized.

Along a ray through focus, which makes an angle θ with the z-axis, we have

$$v = |u|\tan\theta/\sin\alpha. \tag{25}$$

#184950 - $15.00 USD Received 5 Feb 2013; revised 19 Mar 2013; accepted 21 Mar 2013; published 28 Mar 2013

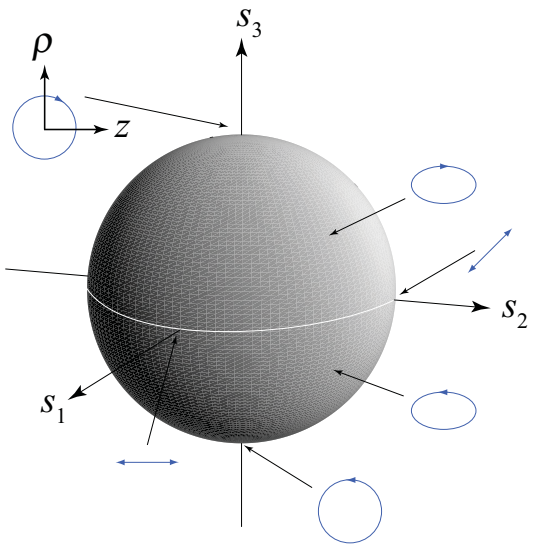

Fig. 5. The Poincaré sphere with Cartesian axes (s_1,s_2,s_3) adapted for focused, radially polarized fields.

From Eqs. (11) and (12) it immediately follows that

$$|e_z(-u,v)| = |e_z(u,v)|, \tag{26}$$
$$|e_\rho(-u,v)| = |e_\rho(u,v)|. \tag{27}$$

These two relations are illustrated in Fig. 6. They also imply that the first Stokes parameter S_0 is an even function in u. Using Eqs. (17) and (19), it is seen that

$$[\delta_z(u,v)-\delta_\rho(u,v)]+[\delta_z(-u,v)-\delta_\rho(-u,v)]=\pi \pmod{2\pi}, \tag{28}$$

for the quantity δ, which is defined below Eq. (24), this implies that $\cos[\delta(-u,v)] = -\cos[\delta(u,v)]$ and $\sin[\delta(-u,v)] = \sin[\delta(u,v)]$. Thus we find the following symmetry relations for the normalized Stokes parameters along a ray through focus:

$$s_1(-u,v) = s_1(u,v), \tag{29}$$
$$s_2(-u,v) = -s_2(u,v), \tag{30}$$
$$s_3(-u,v) = s_3(u,v). \tag{31}$$

An example is presented in Fig. 7. It is seen that S_0, S_1 and S_3 are even, whereas S_2 is odd.

The polarization ellipse may be characterized by two angular parameters (see Fig. 8). One is the orientation angle, ψ ($0 \le \psi < \pi$), which is the angle between the z-axis and the major axis of the polarization ellipse. The other is the ellipticity angle, χ ($-\pi/4 \le \chi < \pi/4$). $|\tan\chi|$ represents the ratio of the axes of the ellipse. The values $\pm\pi/4$ correspond to circular polarization; whereas the value 0 indicates linear polarization. The sign of χ distinguishes the two senses of handedness, i.e., it is right-handed when $\chi > 0$, and left-handed when $\chi < 0$, see [24, Sec. 1.4]. The two angular parameters can be expressed in terms of the normalized Stokes parameters, as

$$\psi = \frac{1}{2}\arctan\left(\frac{s_2}{s_1}\right), \tag{32}$$
$$\chi = \frac{1}{2}\arcsin(s_3). \tag{33}$$

#184950 - $15.00 USD Received 5 Feb 2013; revised 19 Mar 2013; accepted 21 Mar 2013; published 28 Mar 2013

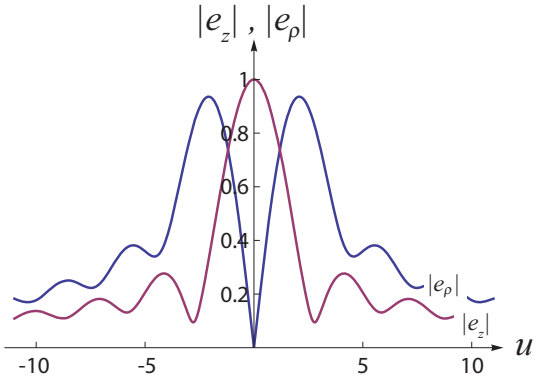

Fig. 6. The normalized moduli of the longitudinal component e_z (red curve) and that of the radial component e_ρ (blue curve) of the electric field along an oblique ray under an angle $\theta = 35^\circ$ with the z-axis. Here we have chosen $\alpha = 40^\circ$ and $\beta = 1$.

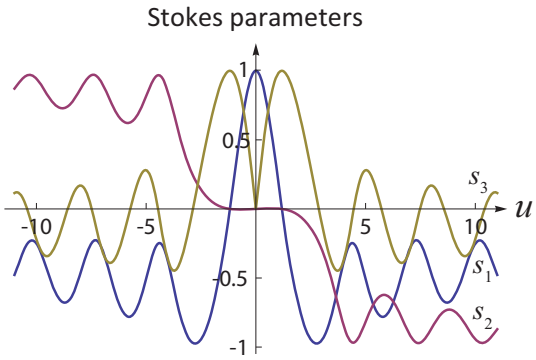

Fig. 7. The Stokes parameters along an oblique ray through focus which makes an angle $\theta = 35^\circ$ with the z-axis (s_1: blue curve, s_2: red curve, s_3: olive curve). Here $\alpha = 40^\circ$ and $\beta = 1$.

From the symmetry relations of s_1, s_2 and s_3, it is seen that

$$\psi(-u,v) = \pi - \psi(u,v), \tag{34}$$

$$\chi(-u,v) = \chi(u,v). \tag{35}$$

Two kinds of polarization singularities can occur. When the polarization ellipse is circular, the orientation angle ψ is undefined. This happens at so-called C-points. When the polarization is linear, the handedness is undefined. This occurs at so-called L-points. When a system parameter, such as the semi-aperture angle α, is varied in a continuous manner, these polarization singularities can be created or annihilated. This has been described in [26, 29].

The curves of the orientation angle ψ and the ellipticity angle χ along an oblique ray under angle $\theta = 35^\circ$ are displayed in Figs. 9 and 10. In Fig. 9 it is seen that the orientation angle of the ellipse oscillates somewhat along the ray. Also, a C-point is seen near $u = \pm 1.2$, where the orientation angle ψ is singular. To the left of the C-point at $u = -1.2$, the polarization ellipse is slightly larger in the ρ-direction than it is in the z-direction. This situation is reversed to the right of that C-point. This coincides with a $\pi/2$ jump of the angle ψ. In Fig. 10, these C-points

#184950 - $15.00 USD Received 5 Feb 2013; revised 19 Mar 2013; accepted 21 Mar 2013; published 28 Mar 2013

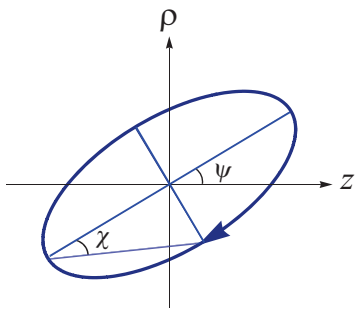

Fig. 8. Defining the angles ψ and χ of a polarization ellipse.

occur when the ellipticity angle χ takes on the value $\pi/4$. When χ equals 0, an L-point occurs, which happens near points such as $u = \pm 2.9$.

In Fig. 11 the polarization ellipse is shown for different positions along an oblique ray. The ellipses at (u, v) and $(u, -v)$ have the same ellipticity and handedness, whereas their orientations are mirror-symmetric. The changes in the polarization ellipse are closely related to the two Gouy phases, as we will now discuss. When $u = -4$, it is seen from Fig. 4 that $\delta = \delta_z - \delta_\rho < 0$, according to Eq. (24) the polarization is then counter-clockwise which corresponds to a point on the southern half of the Poincaré sphere. Near the point $u = -2.87$, $\delta_z = \delta_\rho$, and hence the field is linearly polarized with its handedness undefined, corresponding to a point on the equator. In the vicinity of the focus, the Gouy phase difference, $\delta_z - \delta_\rho$, is approximately $\pi/2$ (see Fig. 4) and when $u = -1.2$ the moduli of the two components attain the same magnitude (see Fig. 6), therefore the field there is circularly polarized, corresponding to a point on the North pole. The field is linearly polarized at focus due to the zero amplitude of the field component e_ρ. We also find that from $u = -4$ to $u = -1.2$ the handedness of the polarization changes from counter-clockwise, to undefined, to clockwise.

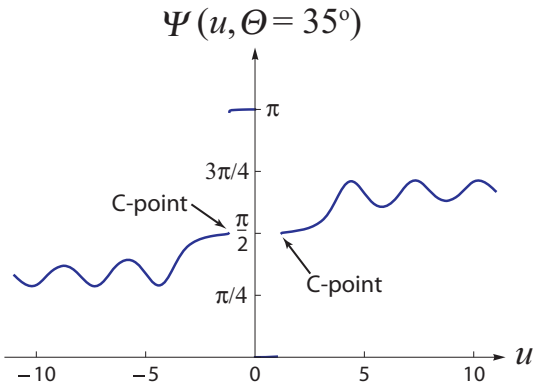

Fig. 9. The orientation angle ψ of the polarization ellipse along an oblique ray through focus under an angle $\theta = 35^\circ$. Here we have chosen $\alpha = 40^\circ$ and $\beta = 1$.

It is seen from Figs. 12, 13, and 14 that the evolution of the polarization ellipse can be quite different along different rays through focus. This behavior mirrors the different Gouy phases that the two components of the electric field vector undergo along these rays. In Fig. 12 (with

#184950 - $15.00 USD Received 5 Feb 2013; revised 19 Mar 2013; accepted 21 Mar 2013; published 28 Mar 2013

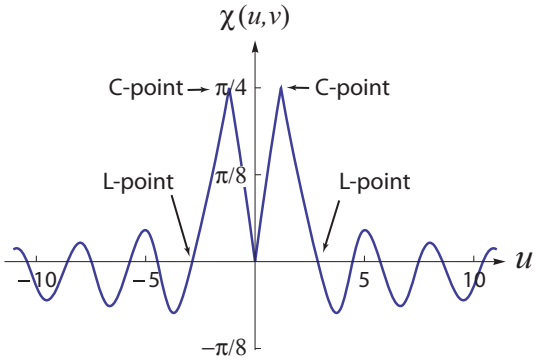

Fig. 10. The ellipticity angle χ of the polarization ellipse along an oblique ray through focus under an angle $\theta = 35^\circ$. Here we have chosen $\alpha = 40^\circ$ and $\beta = 1$.

$\theta = 10^\circ$) the handedness is clockwise at all observation points. This means that the Stokes parameter $s_3 > 0$, i.e. $\delta_z - \delta_\rho > 0$. From Eq. (24) we see that this implies that the relative change of the two Gouy phases is limited along this ray. This is also the case for $\theta = 20^\circ$, as can be seen from Fig. 13. In that case, however, the ellipticity is considerably larger. If the obliquity angle θ is further increased to 30° (see Fig. 14), the polarization ellipses becomes even narrower. In addition, the handedness evolves from counter-clockwise to clockwise, reflecting the fact that $\delta_z - \delta_\rho$ changes sign along the ray. Finally, the change in the orientation angle of the ellipses is seen to decrease significantly when the angle θ is increased.

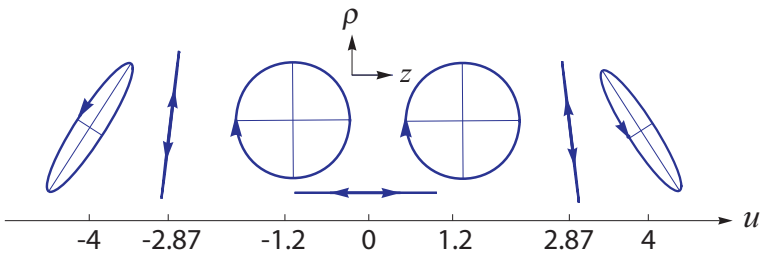

Fig. 11. Illustration of the symmetry properties of the polarization ellipse. The electric field ellipse is shown at selected points along an oblique ray through focus. The ray is under an angle $\theta = 35^\circ$. Also, $\alpha = 40^\circ$ and $\beta = 1$.

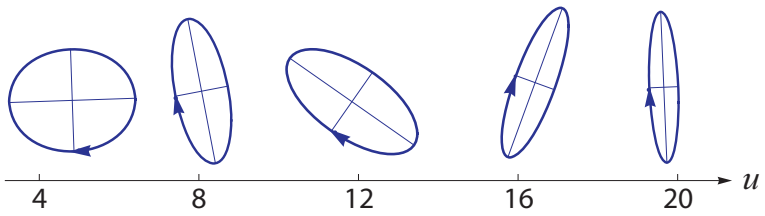

Fig. 12. Polarization ellipse of the field at selected points along an oblique ray through focus. The ray is under an angle $\theta = 10^\circ$. Also, $\alpha = 40^\circ$ and $\beta = 1$.

#184950 - $15.00 USD Received 5 Feb 2013; revised 19 Mar 2013; accepted 21 Mar 2013; published 28 Mar 2013

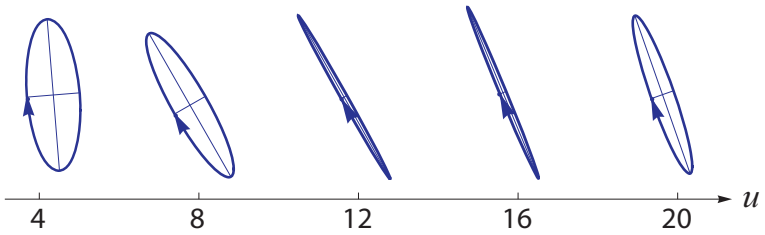

Fig. 13. Polarization ellipse of the field at selected points along an oblique ray through focus. The ray is under an angle $\theta = 20^\circ$. Also, $\alpha = 40^\circ$ and $\beta = 1$.

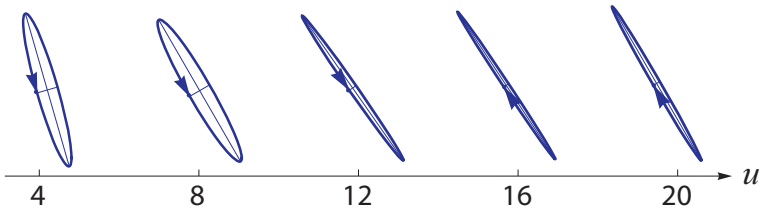

Fig. 14. Polarization ellipse of the field at selected points along an oblique ray through focus. The ray is under an angle $\theta = 30^\circ$. Also, $\alpha = 40^\circ$ and $\beta = 1$.

5. Conclusions

We have analyzed the phase behavior of strongly focused, radially polarized fields. We found that the Gouy phase of the two components of the electric field are quite different, and have different symmetries. Our results show that the semi-aperture angle α and the beam-size parameter β can both influence the Gouy phase. If we follow the polarization ellipse along a tilted ray through focus, it is seen to "tumble", i.e., it changes its orientation, its shape and its handedness. This behavior is due to the different Gouy phases that the two components of the electric field undergo.

#184950 - $15.00 USD Received 5 Feb 2013; revised 19 Mar 2013; accepted 21 Mar 2013; published 28 Mar 2013